Superbroadening in H_2O and D_2O by self-focused picosecond pulses from a YAlG:Nd laser*

W. Lee Smith,† P. Liu, and N. Bloembergen
Gordon McKay Laboratory, Harvard University, Cambridge, Massachusetts 02138
(Received 27 January 1977)

The dielectric breakdown intensity threshold, the critical power for self-focusing, and the power threshold for the production of spectral superbroadening have been measured in H_2O and D_2O. For bandwidth limited pulses of 30 psec duration at 1.06 μm, and 21 psec duration at 0.53 μm, the superbroadening in water always required power levels sufficient for catastrophic self-focusing and intensities equal to the electric breakdown threshold.

I. INTRODUCTION

Frequency broadening of laser pulses was first observed in self-focused filaments in CS_2 and other Kerr-effect liquids.[1-4] The effect is described in the frequency domain as a four-wave parametric interaction which leads to high-order side bands.[3,5] The effect is modulated by contributions from the stimulated Raman effect. In the time domain the effect is described as self-phase modulation.[6] An excellent review with extensive references to literature up to 1971 has been given by Akhmanov *et al.*[7]

Superbroadening with frequency shifts exceeding several thousands of wave numbers can be induced in many materials by sufficiently powerful picosecond pulses, as was first demonstrated by Alfano and Shapiro.[8] The effect can create in a picosecond pulse a quasicontinuum of light from the ultraviolet throughout the visible. Such pulses are used as a source in time-resolved spectroscopy with chemical and biochemical applications.[9]

Investigations of superbroadening in a variety of media have been reported.[8-14] The effect occurs in glasses, alkali halides, and other transparent crystals. In solids it is usually accompanied by filamentary damage tracks created by moving self-focused spots. Damage in liquids is, of course, self-healing, and water is an ideal source for "white" picosecond pulses. The four-wave parametric interaction[15] and the stimulated Raman effect[16] in water have been studied, and it has recently been reported[17] that the self-broadening in D_2O is more pronounced than in H_2O.

In another series of experiments Penzkofer *et al.*[18-20] reported that the intense superbroadening in water (as well as in other materials) does not require the formation of self-focused filaments, and may be explained solely by four-wave parametric instabilities. It is nevertheless clear from our experiments that the required intensities lie uncomfortably close to the breakdown threshold of the transparent materials.

It is the purpose of this paper to report on a careful quantitative comparison of the intensity threshold required for breakdown, on the critical power required for catastrophic self-focusing, and on the threshold for the onset of superbroadening in H_2O and D_2O. In Sec. II the experimental method and results are presented, while in Sec. III a critical comparison of our results with theory and a discussion of the results of previous investigations is given. A brief final section summarizes the conclusions.

II. EXPERIMENTAL METHOD AND RESULTS

Quantitative measurements near breakdown intensities require carefully controlled pulses. We have used single pulses from a mode-locked YAlG:Nd oscillator-amplifier system, previously used in breakdown experiments.[21] The reproducible pulses are Fourier-transform limited and have Gaussian spatial and temporal character. Most experiments were carried out at 1.06 μm with 30-psec pulses, but the frequency dependence of breakdown and superbroadening was checked in pulses at 0.53 μm with 21-psec duration, obtained by frequency doubling in a 90° phase-matched crystal of cesium dihydrogen arsenate. A Glan prism is used after the doubling crystal to eliminate the 1.06-μm radiation. Single pulses, with measured duration, area, and energy, were focused into a cell of H_2O or D_2O. The two liquids were contained in identical cells, 2.5 cm in diameter by 30 cm in length with quartz windows. The commerical D_2O (<0.25% H_2O or HDO) was filtered with 2-μm filter paper before use. The H_2O sample was demineralized, deionized, and then doubly distilled. The linear absorption coefficient at 1.064 μm was measured with a Cary 14 ratio spectrophotometer and found to be 0.13 cm^{-1} for H_2O and less than 0.005 cm^{-1} for D_2O. Because of the linear attenuation in H_2O, the focal plane was located only 5 mm from the entrance window inside the liquids. This distance was mea-

sured accurately so that the actual reduced focal-point intensity could be calculated. All data presented here have been corrected for the linear attenuation and refer to focal-plane values.

A. Dielectric breakdown thresholds

With each material four different lenses were in turn used to focus the calibrated laser pulses 5 mm into the liquid samples to induce breakdown. The lenses had focal length f (and calculated focal area[21]) of 2.54 cm (39.4 μm^2), 3.81 cm (88.5 μm^2), 7.62 cm (353.0 μm^2), and 30.48 cm (5621.0 μm^2). Here the focal area is defined as πw^2, where w is the $1/e$ radius of intensity in the focal plane. For each lens the input power threshold (P_B) for production of a spark at the focal point, detected by dark-adapted 10-in. distant eyes in a dark room, was determined in the same manner as for our previous breakdown studies.[21] (The P_B values are tabulated in Table I.) The reciprocal P_B values are then plotted versus respective reciprocal area (A) for each material, as shown in Fig. 1. From the slope of the line defined by the two data points for the two smallest focal-length lenses,[22] we obtain the reciprocal of the threshold breakdown rms intensity (I_B). The threshold intensity I_B is related to the threshold rms electric field E_B via $I_B = E_B^2 n \epsilon_0 c$, where n is the linear refractive index (taken as 1.33 here for H_2O and D_2O), ϵ_0 is the permittivity of free space, and c is the vacuum speed of light. The threshold quantities I_B and E_B are automatically corrected for self-focusing by this technique.

Results for SiO_2 are compared with those for H_2O and D_2O in Fig. 1. A previously examined SiO_2 sample[21] was retested in the present experiment to check the accuracy of the new calculated focal areas and energy calibration. The E_B value obtained for SiO_2 agrees with the earlier value to within 8%, thereby verifying the accuracy of the experimental parameters and allowing us to compare the present E_B values with those of other materials.[21] The newly measured I_B and E_B values of H_2O and D_2O for 1.064-μm 30-psec pulses, are found in Table II. The experimental accuracy of the E_B values is ±15%. The breakdown threshold field for H_2O is 40% greater than that for D_2O.

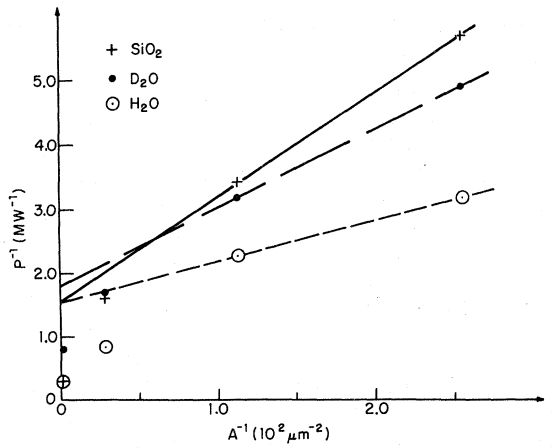

FIG. 1. Plot of reciprocal input power at breakdown threshold vs the reciprocal of the focal areas. The slope of the straight line gives the breakdown threshold electric field and the intercept with the y axis, the critical power for self-focusing (Ref. 23).

In the experiments at the doubled frequency, the focal area is smaller by a factor of 2, and the pulse duration is shorter by a factor $2^{1/2}$. The critical power P_1 for self-focusing at 0.53 μm is four times less than at 1.06 μm. The input power levels for breakdown at 0.53 μm were not sufficiently small compared to P_1 to permit a precise determination of the threshold values E_B, but these are definitely somewhat higher than the E_B values at 1.06 μm.

B. Critical power for self-focusing

The paraxial critical power for self-focusing, denoted P_1, is given by $c\lambda^2/32\pi^2 n_2$, where λ is the light wavelength in vacuum and n_2 is the nonlinear refractive index.[23] From the construction of Fig. 1, P_1 is obtained as the reciprocal of the intercept of the straight line with the P^{-1} axis. The extracted P_1 values are listed in Table II. The quan-

TABLE I. Observed power thresholds necessary to produce breakdown P_B and superbroadening P_{SB} in H_2O and D_2O for lenses of different focal lengths by 30-psec pulses at 1.06-μm wavelength.

	f (cm)	2.54	3.81	7.62	30.48
H_2O	P_B (MW)	0.32	0.44	1.19	3.32
	P_{SB} (MW)	15.67	7.21	4.07	3.32
D_2O	P_B (MW)	0.20	0.31	0.60	1.25
	P_{SB} (MW)	18.80	10.03	4.70	3.13

TABLE II. Values for the breakdown threshold intensity I_B, and field strength E_B, the critical powers for self-focusing and the nonlinear index coefficient n_2 in H_2O and D_2O.

	I_B (TW/cm²)	E_B (MV/cm)	P_1 (MW)	P_2 (MW)	n_2 (10^{-13} esu)
H_2O	1.60	21.3	0.63	2.34	1.7
D_2O	0.82	15.2	0.54	1.99	2.0

tity P_2 in Table II is equal to $3.7P_1$, and is the "catastrophic" critical power for self-focusing.[23] In a focused geometry an input power of P_2, numerically determined, results in a blow-up in axial intensity near the focal point due to whole-beam self-focusing. The actual upper limit to the light intensity sustainable in a material is, of course, set by the breakdown threshold, which sets a lower limit to the filament diameter in catastrophic self-focusing.[24] For lenses with focal area sufficiently large, the power P_B required to induce breakdown will be larger than P_1. Such points will fall below the straight line corresponding to the constant-shape approximation in Fig. 1. When P exceeds P_2, a self-focused filament will always develop in a sample of sufficient length, even without an external lens. Breakdown will always occur for $P>P_2$. The experimental P_B values in Table I with the longest focal length lens are 5.3 and 2.3 times for H_2O and D_2O, respectively, larger than the P_1 values from the constant-shape approximation construction in Fig. 1. Considering the ±50% uncertainty in our P_1 values, the 5.3 factor (>3.7) is not problematic but may indicate simply that the true P_1 value for H_2O is less than 0.63 MW.

The final column of Table II lists the n_2 values obtained from the P_1 measurements. The experimental uncertainty in our n_2 values is also ±50%. Two previous values of n_2 for H_2O have been reported: 0.9×10^{-13} esu (Ref. 25) and 2.5×10^{-13} esu.[20] Our value falls between those two. The value for D_2O is found to be the same within the limits of error.

C. Superbroadening thresholds

The threshold for the production of superbroadened light by 1.06-μm laser pulses was measured with the same experimental arrangement described above for the E_B determinations. The 1.064-μm laser pulse propagated through the cell and onto a white card. The superbroadening threshold was identified by the ocular observation of visible light on the card in a dark room. Our experiments showed that in both H_2O and D_2O for each lens the superbroadening (SB) input power threshold (P_{SB}) was equal to or exceeded both P_B and P_2, as shown in Table I. In such a power regime, it is not useful to speak in terms of *intensity* produced in the sample because, in *all* cases where $P>P_2$, catastrophic self-focusing occurs and the intensity will reach, but not exceed, the breakdown intensity.

The P_{SB} data in Table I clearly show that *strong breakdown indeed occurred* in these liquids during every production of superbroadening. The breakdown sparks were up to 1 cm long at the power levels for superbroadening. The factor by which P_{SB} exceeds P_B in Table I depends strongly on lens focal length l_f, varying between about 1–2.5 for $l_f=30.5$ cm to about 50–90 for $l_f=2.54$ cm. This strong variation of P_{SB}/P_B with focal length indicates the need for breakdown (or near breakdown) intensities to be achieved over at least a minimum distance along the propagation axis. A minimum self-focused *interaction length* is needed for SB to occur. Although the breakdown thresholds were very sharp (<10% uncertainty in P_B), the P_{SB} values were inherently more statistical. This is probably also connected with detailed track geometry of the moving focal spots.

The P_{SB} values in Table I represent power levels of approximately 50% probability for SB. A decrease in input power P of (10 to 20)% typically extinguished all SB. Yet for numerous pulses with power between P_{SB} and ~$3P_{SB}$, no SB was observed. And for most pulses with $P\gtrsim 5P_{SB}$, a massive breakdown spark (~1 mm diam×15 mm long) occurred without producing SB. This behavior points to a delicate balance involving the need for intensification to be achieved over the threshold length, but without the production of a breakdown spark so wide that the laser pulse suffers absorption and reflection over most of its transverse area.

Numerical studies[23] of spatially Gaussian pulse distortion by self-focusing indicate that the transverse distribution becomes drastically sharper as P exceeds P_2. Such radial sharpening would allow whole pulse attenuation by a breakdown plasma. When SB sets in just above the threshold value, the pulse distortion and attenuation is less severe. Breakdown would then occur over a smaller fraction of the transverse area of the pulse,[26] allowing light in the radial wings to propagate past the breakdown plasma and into the post-focal SB amplification region.

Superbroadening power thresholds were also measured at 5321 Å. Output radiation was filtered (Corning 2-63 filter) to remove the 5321-Å component and then displayed on a white card. The SB thresholds were determined by visual observation of Stokes-shifted light. The 5321-Å data is similar to the ir data in several respects. Breakdown occurred at input power levels *several times lower* than the P_{SB} values for the two shortest focal length lenses (only two were used to study breakdown at 5321 Å). The 5321-Å P_{SB} values of H_2O and D_2O for the 30.5-cm lens were about 1.6 and 1.5 MW, respectively, again forming the ratio of ~1.1 as did the corresponding 1.06-μm P_{SB} and P_2 values. The P_{SB} values for the 30.5-cm lens decreased by a factor 2.1 at the second-harmonic

wavelength. Self-focusing theory predicts a greater decrease, by a factor 4, in the quantity P_2, indicating that self-focusing is only one factor in the production of SB.

The superbroadened light has the same polarization as the input laser light. The measured pulse duration of the SB light was always of subnanosecond duration and does not include significant plasma recombination light. This is further confirmed by the angular distribution of the SB light.

D. Spatial and spectral distribution of superbroadened light

The spatial pattern of the SB light was recorded by placing film holders after the sample cell. Single shot exposures were obtained with Kodak EHB color film. The spectral character of the SB light was recorded by focusing the full output from the cell onto the slits of a Spex $\frac{3}{4}$-m spectrometer. Appropriate filters, to remove the pump light or to prohibit multiple-order artifacts, were used between the cell and imaging lens. Kodak 410, 413 infrared, and 1-N plate films (sensitivity range ~9200 Å to below 3000 Å) were used to record single-pulse and accumulated spectra.

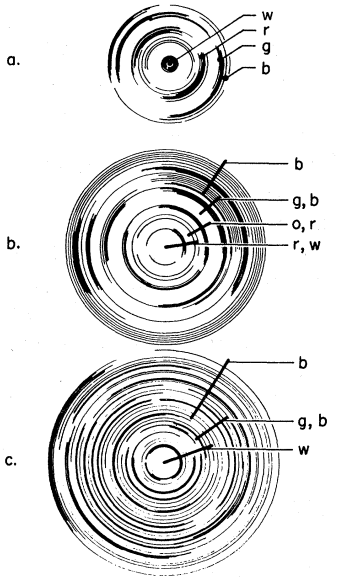

FIG. 2. Spatial distribution of superbroadened light in D_2O in the plane normal to pulse propagation axis. These artist's tracings were derived from color exposures of single shots. The dots or bars indicate spectral content with the notation: w, white; b, blue, g, green; ϕ, orange; r, red. (a) Pattern at SB threshold. (b) Pattern at twice SB threshold. (c) Pattern at saturation (about five times threshold). (A color reproduction has appeared on the cover of the February 1977 issue of Laser Focus.)

Figure 2 exhibits three tracings (in black and white) of single shot exposures (on Kodak EHB film) taken near SB threshold, above threshold, and at saturation. Dots or radial line segments are used in Fig. 2 to indicate the radial distribution of SB wavelengths. The visible onset of SB of 1.06-μm pulses in D_2O was signaled by the appearance of concentric rings of light with wavelengths centered at about 6800 and 5700 Å, sometimes with a third outer blue ring at about 4050 Å. Figure 2(a) is typical of SB threshold. Spectrographic recording located other bands at 3800, 7300, 7750, and 8400 Å. The red, green, and blue rings (spectral width ~200 Å each) at SB threshold were spatially narrow and nonoverlapping, with ring diameter increasing roughly according to photon energy—strongly reminiscent of stimulated Raman scattering (SRS). In fact, the 8400-, 7750-, 6800-, and 5700-Å bands are located at Raman anti-Stokes bands of (gaseous) D_2O, but the 7300-Å band is not.[27] In addition to the anti-Stokes shifted rings, the intense Stokes components coincided with a small bright white disk at the center of the pattern. The behavior in H_2O was similar, with due account for different Stokes shifts.

At threshold, the spatial ring structure fluctuated in diameter, width, uniformity, and concentricity. Occasionally the ring pattern was composed of a major ring system with one or more weaker systems offset. This fluctuant behavior is indicative of the influence of the self-focusing dynamics and plasma buildup, which differ from shot to shot. As the input intensity was raised above SB threshold, the system of separated rings evolved into a "circular rainbow" of color, with radius increasing with photon energy. The entire visible spectrum was produced, as indicated in Fig. 2(b). As the input intensity was raised still higher ($\gtrsim 3P_{SB}$), each ring of a particular color was filled in until, at saturation, each color appeared as a solid disk with disk diameter increasing with photon energy (as observed with various color filters placed after the cell). The superposition of the spectral disks resulted at saturation in a pattern of white central area, fading into a blue outermost rim [Fig. 2(c)].

Qualitative measurements of the spectral content were made with the spectrometer for both 1.06-μm and 5321-Å input pulses. For 1.06-μm input light, the spectral bands mentioned above melded into a rather smooth anti-Stokes continuum which extended for D_2O (H_2O) all the way from 1.06 μm (as detected with overexposed type 413 infrared film) to 3400 Å (4300 Å). No abrupt weakening of the conversion efficiency was observed for SB wavelengths shorter than 5321 Å

(1.06-μm input wavelength). For 5321-Å input radiation, the SB spectrum exhibited more structure both for D_2O and H_2O. The dominant conversion was into the first Stokes band, centered in D_2O (H_2O) at about 6050 Å (6350 Å). A dip in conversion efficiency due to the inverse Raman effect[1] was observed at 4650 Å (4550 Å) in D_2O (H_2O). In the forward direction the long- (short-) wavelength extent of the SB continuum was about 8700 Å (3000 Å) in both liquids.

In our single-pulse spectrograms (if not overexposed) small-scale spectral modulation was always observed. An example is shown in Fig. 3. Such structure has been widely reported and discussed[5,6,12] in terms of self-phase modulation due to a time-dependent index of refraction. In our present case, this modulation is further evidence for the strong influence of self-focusing and breakdown on the production of superbroadened light under our experimental conditions.

III. DISCUSSION

A. Comparison with other experimental results

For the experimental conditions reported in this paper, the occurrence of superbroadening is always preceded by dielectric breakdown and catastrophic self-focusing. These observations appear to be at variance with the findings reported in a series of recent papers[18-20] by Penzkofer *et al.* on superbroadening. It should be kept in mind that in these other experiments pulses from a Nd-glass laser were used with an envelope duration of 6 psec. It is worthwhile to scrutinize the evidence, on which the claim[20] is based, that superbroadening in water is caused solely by four-wave parametric interactions in the absence of breakdown and self-focusing.

Penzkofer *et al.* only state intensity thresholds and do not report data on input power, input area or focal area. Their examination of the intensity distribution on the output face of the sample cell did not reveal any evidence for self-focusing. We do not consider this a good criterion. Only a small fraction of the total pulse energy may have participated in self-focusing, and the light in filaments may already have been diffracted by the time it reached the exit window. For further discussion a reasonable range of diameters for the input beam is assumed. The actual power levels may then be computed from the quoted intensities. A typical input radius, where the intensity has dropped to $1/e$ from its value on axis, may lie in the range of 1.5–4 mm. The focal areas for lenses with focal lengths of 5, 40, and 60 cm, respectively, would lie in the ranges from 100–14.1 μm^2, 6400–900 μm^2, and 14 500–2000 μm^2. These figures neglect linear aberrations and assume a Gaussian single spatial mode. Multimode operation would make our argument even more cogent. Consider the data presented on p. 266 of Ref. 19. The SB threshold for H_2O with the $f=60$-cm lens occurs at an intensity of 2×10^{10} W/cm^2. With the focal area values quoted above, the required input power in this case would lie between 0.4 and 2.9 MW. From our measurement of P_1 in H_2O (see Table II), even the lower limit of 0.4 MW is much too near P_1 to allow one to neglect incipient self-focusing. The upper P limit of 2.9 MW exceeds the *catastrophic* self-focusing critical power P_2—the input power which would produce breakdown in the sample. For the $f=40$-cm data for H_2O on p. 266 of Ref. 19, input powers of 7.2–51.3 MW are indicated. These exceed P_2 by far and virtually assure the formation of self-focused filaments with concomitant breakdown plasma production. For the $f=5$-cm H_2O data likewise all three stated intensity levels[19] are lower than the levels actually reached in the samples. The data entry at 1.4×10^{13} W/cm^2 there indicates an input power between 1.9 and 14.0 MW—again sufficient to induce catastrophic self-focusing.

Penzkofer *et al.* also state that they found no evidence for plasma formation. They employed a method of breakdown detection based on the production of a spot on Polaroid film. We have ascertained that this method is less sensitive than our procedure[21] and would allow breakdown to remain undetected just above threshold. The E_B for 6-psec pulses should be at least twice as large as our $E_B=21.3\pm3.2$ MV/cm for 30-psec pulses, or approximately 5×10^7 V/cm ($I_B\approx1\times10^{13}$ W/cm^2). The input power P_{in} necessary to reach that intensity can be obtained from the relation[21]

$$P_{in}=I_BA/[1+(I_BA/P^*)] \ , \qquad (1)$$

where $P^*=P_1$ or P_2 to obtain the upper and lower limits on P_{in}. Taking into account also the possible range in focal area A, we obtain an upper limit on P_{in} of 0.85 to 1.7 MW (using $P^*=P_2$) and lower limit of 0.42–0.57 MW (using $P^*=P_1$). These input powers required for breakdown lie within the range of input powers we estimated for the super-

FIG. 3. Spectrogram of SB light produced in D_2O by 1.06-μm light. The small-scale modulation period is $\lesssim10$ Å. Film: Polaroid 410; filtration: Corning 3-72; spectral resolution: ~10 Å.

broadening threshold for each of the focal lengths used in the experiments of Ref. 19.

Similar results are found upon examination of the NaCl data reported in Table II of Ref. 19. For example, the SB threshold entry for the 60-cm lens (single pulse) implies an input power of between 0.2 and 1.4 MW, exceeding P_1 ($\approx$0.15 MW) and probably P_2 ($\approx$0.57 MW) for this material.[21]

An additional difference between our observations and the discussion in Ref. 20 involves the phase-matching angle for SB radiation. Figure 3 of Ref. 20 indicates a somewhat larger ϕ, about 6 deg, for red wavelengths, with ϕ then decreasing with decreasing photon wavelength to about 5200 Å (the limit of their calculation). This prediction, resulting from a four-photon parametric generation calculation, is in clear disagreement with the output SB distribution which we have observed.

More-significant linear absorption at 1.06 μm in H_2O than in D_2O appears to be responsible for the observation[17] that superbroadening is more efficient in D_2O.

Other experiments,[8-14] all carried out with Nd-glass lasers, were generally of a more qualitative character. All those experiments are consistent with the statement that superbroadening in water, glass, and alkali halides requires the presence of self-focused filaments and electric breakdown. The different conclusion by Penzkofer *et al.* is based on evidence which in our judgment is not convincing. The question must now be examined of how the different experimental results relate to theoretical models for SB.

B. Comparison with theory

Penzkofer *et al.* have concluded[18-20] that their findings can be explained solely on the basis of four-wave parametric instabilities. The basic process is one in which two laser quanta are transformed into a pair of quanta with conservation of energy $2\omega_l \rightarrow \omega_i + \omega_j$, and momentum $2\vec{k}_l \rightarrow \vec{k}_i + \vec{k}_j$. The observed spectral and angular distribution could be correlated with infrared dispersive resonances in water in a suggestive manner. Several other facts listed below indicate, however, that four-wave parametric mixing is not the sole process, although it is undoubtedly a contributing factor and may well be responsible for spectral detail.

(a) The spectral intensity of SB does not show a significant sudden drop at $2\omega_L$. This would be expected because higher frequency would either require a two-stage or a higher-order parametric mixing process.

(b) The gross characteristics of superbroadening, in terms of intensity and spectral range, in water are very similar to those of NaCl and other materials. The detailed infrared dispersion does not appear to play a dominant role, since NaCl has no infrared absorption features at energies higher than 800 cm^{-1}.

(c) The SB induced in water by 0.53-μm incident radiation is not radically different from that by 1.06-μm radiation. The use of green light has the advantage that generation of Stokes-shifted light can be observed and measured, while the Stokes light generated by 1.06 μm is absorbed.

(d) A parametric instability driven above threshold would tend to sharpen its features. The pair of frequencies $\omega_i + \omega_j$ with the lowest threshold would tend to grow at the expense of all other pairs. All observations point, however, to an ever more diffuse spectral broadening as the power level is increased above the SB threshold.

It is believed that all these features can be explained quite naturally if one admits that catastrophic self-focusing precedes superbroadening, as our experiments indicate. The variation of index of refraction due to plasma formation on the time scales characteristic for the intensity profiles in moving focal spot is so rapid that self-phase modulation can explain the large frequency shifts, as first suggested by Bloembergen.[28] Furthermore, the frequency broadening to the anti-Stokes side should extend farther than to the Stokes side. In the experiments at incident wavelengths of 532 nm (18 793 cm^{-1}) the Stokes side is not absorbed and accessible to observation. The Stokes broadening extended roughly 7300 cm^{-1}, while the anti-Stokes broadening exceeded 14 500 cm^{-1}.

Plasma formation without catastrophic self-focusing does not lead to sufficiently rapid index variations even for pulses of 20 psec duration. Breakdown is observed in the focal area of external lenses at power levels insufficient to produce either self-focused filaments or superbroadening. In this case neither is the time scale sufficiently short nor the interaction length sufficiently long in the plasma breakdown region. The time scale in the self-focused filaments is one to two orders of magnitude shorter, 10^{-13}–10^{-14} sec, and a longer interaction length is also available.[28] In our experiments the spectral intensity also shows periodic variations characteristic of self-phase modulation.

The light is initially generated parametrically by the temporal variation of the $n(t)$ of the plasma. There is no intrinsic threshold for the phase modulation, but there is a threshold for filament and plasma formation. The broad spectrum thus generated escapes from the filaments and is, of course, further amplified and modulated by the contributions to $\chi^{(3)}$ of the host liquid. Four-wave

parametric processes and Raman processes appear to be comparable in importance in the case of water. It is understandable that several Raman transitions contribute to the gain characteristics. Three Raman resonances were discernible in the spectral broadening of D_2O, whereas usually one Raman resonance is dominant in a pure stimulated Raman process.

The angular wave vector and frequency characteristics of the light emitted at an angle to the forward direction are, of course, largely determined by the phase-matching conditions in the host material. Under the conditions of our experiment the anti-Stokes Raman processes appeared to play a dominant role in the observed angular spectral dependence. A phase-matching calculation based on four-wave parametric processes and the known infrared dispersion of water could not explain our observations, although it may play an important role under other conditions.

A superbroadened spectrum is also generated in a medium such as liquid argon.[29] In this case Raman processes and infrared dispersion are obviously not important. Even in liquid argon there may still be some nonresonant four-wave parametric mixing of the light initially generated by phase modulation of the plasma index in the self-focused filaments.

Finally, attention is called to another estimate of the self-focusing threshold by Campillo *et al.*,[30] who use a formula for the distance of so-called small scale self-focusing

$$Z_f = \frac{10^{-7} c n_0}{6\pi n_2} \frac{c/\omega}{I} \log_{10}\left(\frac{3}{\delta}\right).$$

Using the parameters given in Penzkofer's experiments ($Z_f = 2$ cm, $n_0 = 1.33$, $n_2 \approx 1.5\times10^{-13}$, and $\delta = 10^{-4}$ as a typical number for small-scale phase perturbations), one finds a threshold intensity for small-scale self-focusing, $I_{th} \sim 5\times10^{10}$ W/cm^2. This value is also very close to the threshold value for superbroadening observed by Penzkofer *et al.*, and again casts doubt on ascribing this threshold to a four-wave parametric process.

IV. CONCLUSION

The production of superbroadening in H_2O and D_2O by 30-psec pulses at 1.06 μm, and 21-psec pulses at 0.53 μm, is preceded by catastrophic self-focusing, filament formation, and breakdown. Self-phase modulation of the rapidly varying index of the plasma provides seed light over a superbroadened spectral interval, which is largely independent of the nature of the host material. This seed light is subsequently further amplified by stimulated Raman gain and four-photon parametric interactions. Both these processes are described by the nonlinear susceptibility $\chi^{(3)}$, characteristic of the host material.

These latter processes lead to a specific angular and frequency dependence of the spectral intensity. Under our conditions the stimulated Raman processes appeared dominant, whereas in other experiments the phase-matching characteristics of four-photon parametric processes determined by the infrared absorption of water played a more important role. The combination of self-phase modulation by plasma formation in self-focused filaments and the $\chi^{(3)}$-process characteristic of the host material can account for and reconcile the different observations by various groups of investigators.

ACKNOWLEDGMENTS

The authors appreciate the assistance of Dr. J. H. Bechtel, now at General Motors Research Laboratory, at an early stage of this work, and thank Professor E. Yablonovitch for a helpful discussion.

*Research supported in part by the Advanced Research Projects Agency of the Department of Defense (and monitored by the Air Force Office of Scientific Research under Contract No. F44620-75-C-0088), by the Joint Services Electronics Program, and by the National Aeronautics and Space Administration.

†Present address: Lawrence Livermore Laboratory, University of California, Livermore, Calif. 94550.

[1]W. J. Jones and B. P. Stoicheff, Phys. Rev. Lett. 13, 657 (1964).

[2]D. I. Mash, V. V. Morozov, V. S. Starunov, and I. L. Fabelinskii, Zh. Eksp. Teor. Fiz. Pis'ma Red. 2, 41 (1965) [JETP Lett. 2, 25 (1965)].

[3]N. Bloembergen and P. Lallemand, Phys. Rev. Lett. 16, 81 (1966).

[4]P. Lallemand, Appl. Phys. Lett. 8, 276 (1966).

[5]A. C. Cheung, D. M. Rank, R. Y. Chiao, and C. H. Townes, Phys. Rev. Lett. 20, 786 (1968).

[6]F. Shimizu, Phys. Rev. Lett. 19, 1097 (1967).

[7]S. A. Akhamnov, R. V. Khokhlov, and A. P. Sukhorukov, *Laser Handbook*, Vol. 2, edited by F. T. Arecchi and E. O. Schulz-DuBois (North-Holland, Amsterdam, 1972), Chap. E3.

[8]R. R. Alfano and S. L. Shapiro, Phys. Rev. Lett. 24, 584 (1970); 24, 592 (1970).

[9]G. E. Busch, R. P. Jones, and P. M. Rentzepis, Chem. Phys. Lett. 18, 178 (1973).

[10]N. G. Bondarenko, I. V. Eremina, and V. I. Talanov, Zh. Eksp. Teor. Fiz. Pis'ma Red. 12, 125 (1970) [JETP Lett. 12, 85 (1970)].

[11]N. N. Il'ichev, V. V. Krobkin, V. A. Korshunov, A. A. Malyutin, T. G. Okroashvili, and P. P. Pashinin, Zh. Eksp. Teor. Fiz. Pis'ma Red. 15, 191 (1972) [JETP Lett. 15, 133 (1972)].
[12]R. R. Alfano, L. L. Hope, and S. L. Shapiro, Phys. Rev. A 6, 433 (1972).
[13]W. Werncke, A. Lan, M. Pfeiffer, K. Lenz, H.-J. Weigmann, and C. D. Thuy, Opt. Commun. 4, 413 (1972).
[14]W. Yu, R. R. Alfano, C. L. Sam, and R. J. Seymour, Opt. Commun. 14, 344 (1975).
[15]D. L. Weinberg, Appl. Phys. Lett. 14, 32 (1969).
[16]J. J. Colles, G. E. Walraven, and K. W. Wecht, Chem. Phys. Lett. 4, 621 (1970).
[17]D. K. Sharma, R. W. Yip, D. F. Williams, S. E. Sugamori, and L. L. T. Bradley, Chem. Phys. Lett. 41, 460 (1976).
[18]A. Penzkofer, A. Laubereau, and W. Kaiser, Phys. Rev. Lett. 31, 863 (1973).
[19]A. Penzkofer, Opt. Commun. 11, 265 (1974).
[20]A. Penzkofer, A. Seilmeier, and W. Kaiser, Opt. Commun. 14, 363 (1975).
[21]W. Lee Smith, J. H. Bechtel, and N. Bloembergen, Phys. Rev. B 12, 706 (1975); and Phys. Rev. B 15, 4039 (1977); W. Lee Smith and J. H. Bechtel, Appl. Phys. Lett. 28, 606 (1976).
[22]The slope-intercept line construction is based on the applicability of the constant-shape approximation, as discussed in the second entry of Ref. 21. Accordingly, in Fig. 1 only data points with $P_B < P_1$ may be used to determine the constructed line.
[23]J. H. Marburger, in *Progress in Quantum Electronics*, edited by J. H. Sanders and S. Stenholm (Pergamon, Oxford, 1975), Vol. 4, Part. 1.
[24]N. Bloembergen and E. Yablonovitch, Phys. Rev. Lett. 29, 907 (1972).
[25]M. Paillette, Ann. Phys. (Paris) 4, 671 (1969).
[26]W. Lee Smith, J. H. Bechtel, and N. Bloembergen, Opt. Commun. 18, 592 (1976).
[27]G. Herzberg, *Molecular Spectra and Molecular Structure* (Van Nostrand, New York, 1964), p. 282.
[28]N. Bloembergen, Opt. Commun. 8, 285 (1)973).
[29]R. R. Alfano and S. L. Shapiro, Phys. Rev. Lett. 24, 1217 (1970).
[30]A. J. Campillo, S. L. Shapiro, and B. R. Suydam, Appl. Phys. Lett. 24, 178 (1974).

FIG. 3. Spectrogram of SB light produced in D_2O by 1.06-μm light. The small-scale modulation period is $\lesssim 10$ Å. Film: Polaroid 410; filtration: Corning 3-72; spectral resolution: ~ 10 Å.